



# Cold plasma treatment triggers antioxidative defense system and induces changes in hyphal surface and subcellular structures of *Aspergillus flavus*

Juliana Šimončicová<sup>1</sup> · Barbora Kaliňáková<sup>1</sup> · Dušan Kováčik<sup>2</sup> · Veronika Medvecká<sup>2</sup> · Boris Lakatoš<sup>1</sup> · Svetlana Kryštofová<sup>1</sup> · Lucia Hoppanová<sup>1</sup> · Veronika Palušková<sup>1</sup> · Daniela Hudcová<sup>1</sup> · Pavol Ďurina<sup>2</sup> · Anna Zahoranová<sup>2</sup>

Received: 5 March 2018 / Revised: 15 May 2018 / Accepted: 19 May 2018 / Published online: 1 June 2018  
© Springer-Verlag GmbH Germany, part of Springer Nature 2018

## Abstract

The cold atmospheric-pressure plasma (CAPP) has become one of the recent effective decontamination technologies, but CAPP interactions with biological material remain the subject of many studies. The CAPP generates numerous types of particles and radiations that synergistically affect cells and tissues differently depending on their structure. In this study, we investigated the effect of CAPP generated by diffuse coplanar surface barrier discharge on hyphae of *Aspergillus flavus*. Hyphae underwent massive structural changes after plasma treatment. Scanning electron microscopy showed drying hyphae that were forming creases on the hyphal surface. ATR-FTIR analysis demonstrated an increase of signal intensity for C=O and C-O stretching vibrations indicating chemical changes in molecular structures located on hyphal surface. The increase in membrane permeability was detected by the fluorescent dye, propidium iodide. Biomass dry weight determination and increase in permeability indicated leakage of cell content and subsequent death. Disintegration of nuclei and DNA degradation confirmed cell death after plasma treatment. Damage of plasma membrane was related to lipoperoxidation that was determined by higher levels of thiobarbituric acid reactive species after plasma treatment. The CAPP treatment led to rise of intracellular ROS levels detected by fluorescent microscopy using 2',7'-dichlorodihydrofluorescein diacetate. At the same time, antioxidant enzyme activities increased, and level of reduced glutathione decreased. The results in this study indicated that the CAPP treatment in *A. flavus* targeted both cell surface structures, cell wall, and plasma membrane, inflicting injury on hyphal cells which led to subsequent oxidative stress and finally cell death at higher CAPP doses.

**Keywords** Antioxidant defense system · *Aspergillus flavus* · Cold atmospheric pressure plasma · FTIR · Lipid peroxidation · Oxidative stress

## Introduction

A plasma is referred to as the fourth state of matter. It is an ionized gas appearing as quasineutral consisting of a large

amount of different species such as charged particles (electrons and ions), free radicals, neutral species (excited atoms and molecules), photons (visible, UV-A, and UV-B), and electromagnetic field (Misra et al. 2011; Mir et al. 2016). Non-equilibrium, the cold atmospheric-pressure plasma (CAPP) is generated, if most of the coupled energy in electrical discharge is transmitted into the electrons and therefore, ions and neutral species of gas remain cold (Ehlbeck et al. 2011). Over the last 20 years, the CAPP has been widely studied for application in medicine, agriculture, and food industry (Misra et al. 2011; Graves 2014; Laroussi 2014; Thirumdas et al. 2014; Mir et al. 2016).

The application of the CAPP in decontamination has become one of the recent ecology friendly technologies. The method is very fast, economically advantageous and suitable for treatment of thermosensitive materials without leaving

✉ Juliana Šimončicová  
juliana.simoncicova@stuba.sk

✉ Barbora Kaliňáková  
barbora.kalinakova@stuba.sk

<sup>1</sup> Institute of Biochemistry and Microbiology, Faculty of Chemical and Food Technology, Slovak University of Technology, Bratislava, Slovakia

<sup>2</sup> Department of Experimental Physics, Faculty of Mathematics, Physics, and Informatics, Comenius University, Bratislava, Slovakia

toxic residues. Many studies have been carried out to inactivate viruses (Su et al. 2018), bacteria (Deng et al. 2006; Roth et al. 2010; Joshi et al. 2011), yeasts (Ryu et al. 2013), filamentous fungi (Zahoranová et al. 2016), and cancer cell lines (Conway et al. 2016).

Depending on the plasma parameters (gas composition, humidity, and temperature), various biologically active agents, such as reactive oxygen species (ROS) and reactive nitrogen species (RNS), UV radiation, visible and infrared radiation, charged particles, electric field, and heat, are generated by the plasma (Deng et al. 2006; Ehlbeck et al. 2011; Misra et al. 2011). The plasma components have been extensively studied (Laroussi and Leipold 2004; Laroussi 2005; Deng et al. 2006) in the context of microbial inactivation. Each of these species can affect microorganisms independently, but it has been shown that decontamination by the plasma is effective primarily due to the synergistic effect of the plasma components which makes the plasma unique (Fridman 2008; Ehlbeck et al. 2011; Bourke et al. 2017). It has been suggested that ROS, RNS, and partly UV radiation could play a key role in microbial inactivation. ROS are involved in oxidative stress, which may result in cellular damage or cell death (Laroussi and Leipold 2004; Deng et al. 2006; Fridman 2008; Jiang et al. 2011; Graves 2014; Arjunan et al. 2015; Bourke et al. 2017). ROS are responsible for triggering many changes within cells such as oxidation of the outer membrane through protein denaturation to breaks of intracellular DNA (Gaunt et al. 2006; Arjunan et al. 2015). The impact of the plasma depends on an organism and its specific cell properties (Mai-Prochnow et al. 2016; Bourke et al. 2017).

In this study, the ascomycete *A. flavus* was selected as a model organism whose genetics and metabolism have been extensively studied for decades (Amaike and Keller 2011; Amare and Keller 2014). *A. flavus* is a saprophytic soil filamentous fungus infecting economically important agricultural crops, such as maize, peanuts, and wheat. In addition, this fungus contaminates crops with dangerous mycotoxins, such as aflatoxin B1 (AFB<sub>1</sub>), one of the most carcinogenic natural compound (Amaike and Keller 2011; Amare and Keller 2014; Šimončicová et al. 2017). Studies have shown that the CAPP can effectively inhibit the growth of *A. flavus* on hazelnuts (Dasan et al. 2016b), different types of grains, legumes (Selcuk et al. 2008; Dasan et al. 2016a), and groundnuts (Devi et al. 2017), and brown rice cereal bars (Suhem et al. 2013). Moreover, the CAPP can be used for degradation or removal of isolated mycotoxins, such as AFB<sub>1</sub>, deoxynivalenol, and nivalenol by microwave-induced argon plasma system at atmospheric pressure (Park et al. 2007). Isolated form of AFB<sub>1</sub> was also detoxicated using nitrogen gas plasma (Sakudo et al. 2017). Influence of the CAPP on aflatoxin production in groundnuts has been investigated recently (Devi et al. 2017). It seems that the CAPP could be used

in detoxification not only aflatoxins but also other dangerous mycotoxins (Hojnik et al. 2017; ten Bosch et al. 2017).

In this paper, we investigated the effect of the diffuse coplanar surface barrier discharge (DCSBD) plasma treatment in ambient air on *A. flavus* mycelium structure, integrity, and redox status. The DCSBD generating CAPP in ambient air was previously described (Černák et al. 2009). The plasma device was primarily designed for treatment of plant matrices, such as seeds (Henselová et al. 2012; Zahoranová et al. 2016). In this study, we explored changes in the antioxidant defense system (antioxidant enzymes activity and non-protein antioxidant production), accumulation of intracellular ROS, changes in cell envelope structures (cell walls, membranes), and macromolecule stability (lipid oxidation and DNA damage) induced by plasma treatment of fungal cells in dose-dependent manner.

## Materials and methods

### Strain maintenance and cultivation

The atoxigenic fungal strain of *A. flavus* CCM F-171 obtained from the Czech Collection of Microorganisms (Masaryk University, Brno, Czech Republic) was used in all experiments. The spores were harvested in 0.1% Tween 80 (Biolife, Milano, Italy) from the 14-day-old cultures grown on malt extract agar (Biolife, Milano, Italy) at 25 °C. The spore suspension was filtered through three layers of sterile gauze and centrifuged at 12,000 ×g for 5 min. The concentration of spores was adjusted by sterile water to  $1 \times 10^9$  spores ml<sup>-1</sup>. Number of spores spread evenly on top of the cellophane membrane (Ø 9 cm) placed on the agar medium was either  $2 \times 10^7$  spores or 20 spores for microscopic observations and cultured in the dark at 37 °C for 16–20 h. These procedures enabled us to obtain fungal samples that were either arranged in homogenous layers of mycelium ( $2 \times 10^7$  spores) or as individual colonies (20 spores).

### Plasma treatment of fungal mycelium

The DCSBD generating CAPP in ambient air was used for the treatment of mycelial samples. The treatment was done at input power 400 W, at which the whole DCSBD ceramic panel is covered with the macroscopically diffuse plasma layer with dimensions 8 × 20 cm and active thickness 0.3–0.5 mm (Černák et al. 2004) and all samples were treated homogeneously. The experimental set-up is depicted in Fig. 1. The temperature of sample was measured by contactless infrared thermometer BaseTech Mini 1 (BaseTech, Dallas, USA).

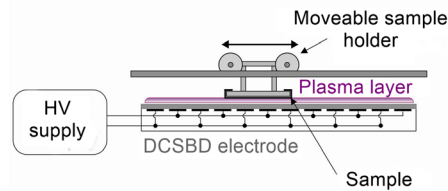
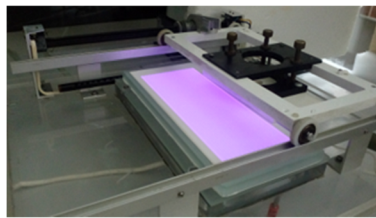


**Fig. 1** Experimental set-up and the schematic draw of diffuse coplanar surface barrier discharge (DCSBD) electrode system. The samples of young mycelium grown on cellophane membrane were placed on the holder of the moving cart facing the ceramic plate of DCSBD creating

0.8-mm distance. The sample passed once through the plasma field (active thickness 0.3–0.5 mm) from one side to the other one with the speed corresponding to the exposure time of 5 s. The total treatment time was achieved by repetition of this procedure (HV, high-voltage)

## Cell viability determination

Plasma-treated mycelium was transferred into fresh malt extract broth (Biolife, Milano, Italy) with chloramphenicol ( $0.1 \text{ mg ml}^{-1}$ ; Thermo Fisher GmbH, Karlsruhe, Germany), and the mycelium was further cultivated on a rotary shaker (120 rpm) at  $25 \text{ }^{\circ}\text{C}$  for 24 h. After cultivation, the mycelium was collected from the culture by vacuum filtration, washed with 50 ml of distilled water, and dried at  $80 \text{ }^{\circ}\text{C}$  to determine biomass weight.

## Scanning electron microscopy

The changes in the cell wall of *A. flavus* hyphae before and after plasma treatment were studied by scanning electron microscopy (SEM) using Vega II SBH (Tescan, Brno, Czech Republic) modified according to Devi et al. (2017). Samples for SEM measurements were coated with the gold by SEM Coating System (BIO-RAD E52-5199, Watford, England) at pressure 8 Pa in argon. The thickness of the gold layer was approximately 20 nm.

## Intracellular ROS detection

The intracellular ROS accumulation in mycelium was determined using 2',7'-dichlorodihydrofluorescein diacetate ( $\text{H}_2\text{DCFDA}$ ; Sigma, Steinheim, Germany). The plasma-treated, and untreated mycelium were dyed immediately by  $\text{H}_2\text{DCFDA}$  ( $0.2 \text{ } \mu\text{mol l}^{-1}$ ) in DMSO (Mikrochem, Pezinok, Slovakia) in the dark at  $25 \text{ }^{\circ}\text{C}$  for 30 min. The stained mycelium was washed three times in phosphate-buffered saline (PBS;  $10 \text{ mmol l}^{-1}$ , pH 7). The intracellular ROS was visualized by fluorescence microscopy (Nikon Eclipse Ti-E/B, Tokyo, Japan) using 495/529-nm excitation and emission wavelengths.

## Determination of cell integrity

The fluorescent dyes, Hoechst 33342 (Sigma, St. Louis, USA) and propidium iodide (PI; Sigma, St. Louis, USA), were used to visualize nuclei or to determine the damage

in the plasma membrane permeability, respectively. Both untreated and treated mycelium by the plasma for 30 and 60 s were incubated with PI ( $1 \text{ } \mu\text{mol l}^{-1}$ ) and Hoechst 33342 ( $5 \text{ } \mu\text{mol l}^{-1}$ ) in dark at  $25 \text{ }^{\circ}\text{C}$  for 30 min. After incubation, the mycelium was washed three times in PBS ( $10 \text{ mmol l}^{-1}$ , pH 7) and observed by confocal microscopy (Nikon Eclipse Ti-E/B, Tokyo, Japan) using 350/461-nm excitation and emission wavelengths for Hoechst 33342 and 535/617 nm for PI.

## Detection of DNA degradation

The DNA from *A. flavus* mycelium was isolated using cell lysis solution (Qiagen, Maryland, USA), protein precipitation solution (Qiagen, Maryland, USA), and proteinase K (Sigma, St. Louis, USA), which were used according to the manufacturer's instructions. Agarose gel electrophoresis was used to demonstrate DNA disintegration. DNA ( $500 \text{ ng } \mu\text{l}^{-1}$ ) from untreated and plasma-treated samples separated by agarose gel electrophoresis stained by GelRed (Biotium, Hayward, USA) and photographed using Amersham<sup>TM</sup> Imager 600 (GE Healthcare Bio Science, Malmö, Sweden).

## Lipid peroxidation assay

The oxidative damage of lipids was quantified by the 2-thiobarbituric acid reactive substances (TBARS) assay modified according to Kiššová et al. (2006). The reagent to detect TBARS was composed of hydrochloric acid ( $1200 \text{ mmol l}^{-1}$ ; Centralchem, Bratislava, Slovakia), trichloroacetic acid ( $734 \text{ mmol l}^{-1}$ ; Merck, Darmstadt, Germany), and 2-thiobarbituric acid ( $26 \text{ mmol l}^{-1}$ ; Merck, Darmstadt, Germany). Sample was treated with the reagent at  $95 \text{ }^{\circ}\text{C}$  for 30 min. The cooled mixture was centrifuged at  $12,000 \times g$  for 10 min, and the absorbance of supernatant was measured at 520 nm (SPECORD-250 Analytic Jena, Jena, Germany). The levels of TBARS were calculated using the molar extinction coefficient for malondialdehyde (MDA)— $156,000 \text{ mol l}^{-1} \text{ cm}^{-1}$ .

## Antioxidant enzyme activity assays

The antioxidant activities of catalase (CAT, EC: 1.11.1.6), superoxide dismutase (SOD, EC: 1.15.1.1), and guaiacol peroxidase (GPX, EC: 1.11.1.7) were measured. For enzymatic assays, 15- and 30-s plasma-treated, untreated mycelium, and mycelium cultivated on culture medium with the addition of H<sub>2</sub>O<sub>2</sub> (0.5 mmol l<sup>-1</sup>; Mikrochem, Pezinok, Slovakia) were freeze-dried in liquid nitrogen and ground to a fine powder. Samples were homogenized in PBS (10 mmol l<sup>-1</sup>, pH 7) containing EDTA (1 mmol l<sup>-1</sup>; Sigma, St. Louis, USA) and phenyl methylsulfonyl fluoride (0.5 mmol l<sup>-1</sup>; GmbM, Mannheim, Germany). Samples were centrifuged in 7000 ×g for 15 min at 4 °C (Centrifuge 5430R, Eppendorf, Hamburg, Germany), and supernatant was used as an enzyme extract.

The CAT activity was measured based on the reduction of dichromate in acetic acid to chromic acetate when heated in the presence of H<sub>2</sub>O<sub>2</sub> according to Sinha (1972). The assay mixture contained PBS (10 mmol l<sup>-1</sup>, pH 7), H<sub>2</sub>O<sub>2</sub> (80 mmol l<sup>-1</sup>) and the cell extract. The reaction was stopped by dichromate (dissolved in water 5% v/v) and mixed with acetic acid (1:3; Centralchem, Bratislava, Slovakia). The samples were incubated at 100 °C for 10 min. The absorbance of chromic acetate was measured at 570 nm (SPECORD-250 Analytic Jena, Jena, Germany). The CAT activity was calculated using calibration curve plotted using known concentrations of H<sub>2</sub>O<sub>2</sub>.

The determination of the SOD activity was based on the competitive reduction of superoxide radicals by *p*-iodonitrotetrazolium (2-[4-iodophenyl]-3-[4-nitrophenyl]-5-phenyltetrazolium) chloride (INT, Sigma, St. Louis, USA). The reaction mixture contained PBS (50 mmol l<sup>-1</sup>, pH 7.8), methionine (19 mmol l<sup>-1</sup>; Sigma, St. Louis, USA), riboflavin (3 μmol l<sup>-1</sup>; Sigma, St. Louis, USA), INT (0.8 μmol l<sup>-1</sup>), EDTA (0.15 μmol l<sup>-1</sup>), and the enzyme extract. After incubation the samples were incubated in the light or in the dark, the absorbance of reduced INT was measured at 490 nm (SPECORD-250 Analytic Jena, Jena, Germany).

The GPX activity was assayed by measuring the oxidation of guaiacol in the presence of H<sub>2</sub>O<sub>2</sub> to tetraguaiacol. The reaction mixture contained PBS (100 mmol l<sup>-1</sup>, pH 5), guaiacol (0.1 mol l<sup>-1</sup>; Cayman Chemical Company, Ann Arbor, USA), H<sub>2</sub>O<sub>2</sub> (10 mmol l<sup>-1</sup>), and the enzyme extract. Reaction was triggered by addition of H<sub>2</sub>O<sub>2</sub>. The GPX activity was determined by measuring increase in absorbance at 470 nm (Ultraspec 7000, GE Healthcare Life Sciences, Loughborough, England) over 15 min.

Activities of antioxidant enzymes were expressed as Unit per mg of proteins. One unit of enzyme activity was defined as amount of enzyme that catalyzed

conversion of one μmol of substrate per min. Concentration of proteins was determined according to Bradford (1976).

## Total reduced glutathione content

The total reduced glutathione (GSH) was measured by the colorimetric method according to Ellman (1959). After homogenization and centrifugation described above, mycelial supernatant was incubated with sulfosalicylic acid (30% w/v; Merck, Darmstadt, Germany) in a ratio of 1:5 for 10 min, followed by centrifugation at 600 ×g for 5 min, and the deproteinized supernatant was collected. The reaction mixture contained PBS (100 mmol l<sup>-1</sup>, pH 8), 5,5-dithiobis-2-nitrobenzoic acid (DTNB; Sigma, Munich, Germany) (721 μmol l<sup>-1</sup>, prepared in buffer) and deproteinized supernatant. GSH formed with DTNB a yellow complex. The absorbance of samples was determined at 412 nm (SPECORD-250 Analytic Jena, Jena, Germany). GSH content was calculated using the standard curve plotted using reduced GSH (Sigma, Tokyo, Japan).

## Fourier-transform infrared spectroscopic analysis

Attenuated total reflectance-Fourier-transform infrared spectroscopy (ATR-FTIR) was used for detection of the changes in specific chemical groups on the surface of *A. flavus* before and after plasma treatment. FTIR spectra were obtained using Bruker Vector 22 FTIR spectrometer with additional accessories Pike MIRacle™ (Optik Instruments, Brno, Czech Republic) in the range of 4000 to 500 cm<sup>-1</sup> during 20 scans, with 4-cm<sup>-1</sup> resolution using diamond crystal.

## Statistical analysis

The data was expressed as a mean ± standard deviation (SD) of at least three replicated measurements. Significant differences between treatments were evaluated using the one-way analysis of variance. Two groups of data were compared statistically by Student's *t* test (Microsoft Excel). Differences were considered significant for *P* value < 0.05.

## Results

### The DCSBD plasma rapidly inhibited growth of *A. flavus* mycelium

The effect of plasma treatment on the vitality of *A. flavus* mycelium grown for 16–20 h on the MEA was determined by measuring dry weight of mycelial biomass after 24-h cultivation in liquid culture medium upon reaching stationary phase (Mohamad et al. 2010). The growth of *A. flavus*

significantly decreased already after a short plasma treatment time (Fig. 2). The treatment with the plasma for 5 s leads to approximately 55% reduction in biomass production in comparison to untreated samples. The decrease of vitality to 10% in mycelial dry weight was observed after 15 s of the plasma treatment. Plasma treatment for 30 s caused the complete or almost complete loss of cell viability. To confirm that the stress induced by cold plasma treatment of samples was not caused by higher temperature, sample temperature was measured immediately after treatment. Temperature of samples treated by plasma for 180 s rose to  $33.1 \pm 1.0$  °C, which is lower than the physiological optimum for *A. flavus*.

### Plasma treatment remodeled cell surface of *A. flavus* mycelium

Changes of the cell wall surface of hyphae after 60- and 180-s plasma treatment were observed by SEM (Fig. 3). The control sample (Fig. 3a, d) appeared to be decompressed, but intact with smooth tubular structure. First differences were detected in the 60-s plasma-treated samples (Fig. 3b, e). Plasma-treated hyphae (Fig. 3b, c, e, f) differ from the untreated by different depressions on the hyphae, which are reflected in retraction and sharp edges present on the surface. The hyphae after plasma treatment were more shriveled and crinkled than the control sample.

### Accumulation of intracellular ROS occurs after plasma treatment

The presence of intracellular ROS generated and accumulated in plasma-treated fungal cells was observed using fluorescent probe H<sub>2</sub>DCFDA (Fig. 4). H<sub>2</sub>DCFDA is stable cell-permeable molecule and it is deacetylated by intracellular esterases to

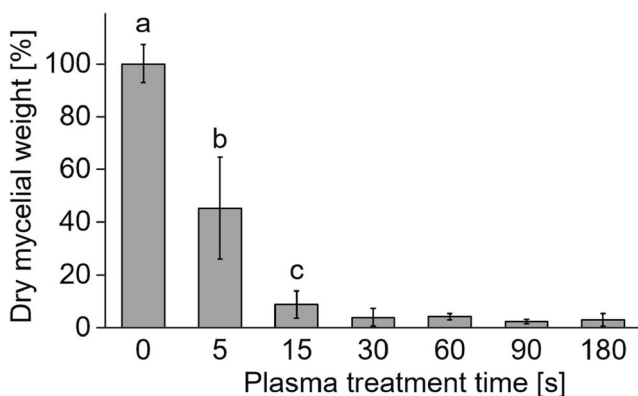


**Fig. 2** Decrease of dry mycelial weight after plasma treatment and subsequent cultivation. Results are presented as a mean  $\pm$  SD ( $n=4$ ). Columns with different letters represent statistically significant results ( $P < 0.05$ ). Cell viability after longer than 30-s plasma treatment was statistically insignificant ( $P > 0.05$ ) compared with viability of the plasma-treated cell for 15 s, but they are statistically significant ( $P < 0.001$ ) in compared to control

non-fluorescence probe 2',7'-dichlorodihydrofluorescein, which is oxidized and converted into highly fluorescent product 2',7'-dichlorofluorescein (DCF) by intracellular ROS. In untreated hyphae, weak green fluorescence signal of DCF was observed (Fig. 4d), which indicated low physiological level of intracellular ROS. On the other hand, significantly increased intensity of DCF fluorescence was detected in plasma-treated hyphae after 30 and 60 s (Fig. 4e, f). In contrast to the plasma-treated hyphae (Fig. 4b, c), vacuoles were observed only in untreated control samples (Fig. 4a).

### Plasma-generated oxidants attack lipids and cause increase in cell membrane permeability

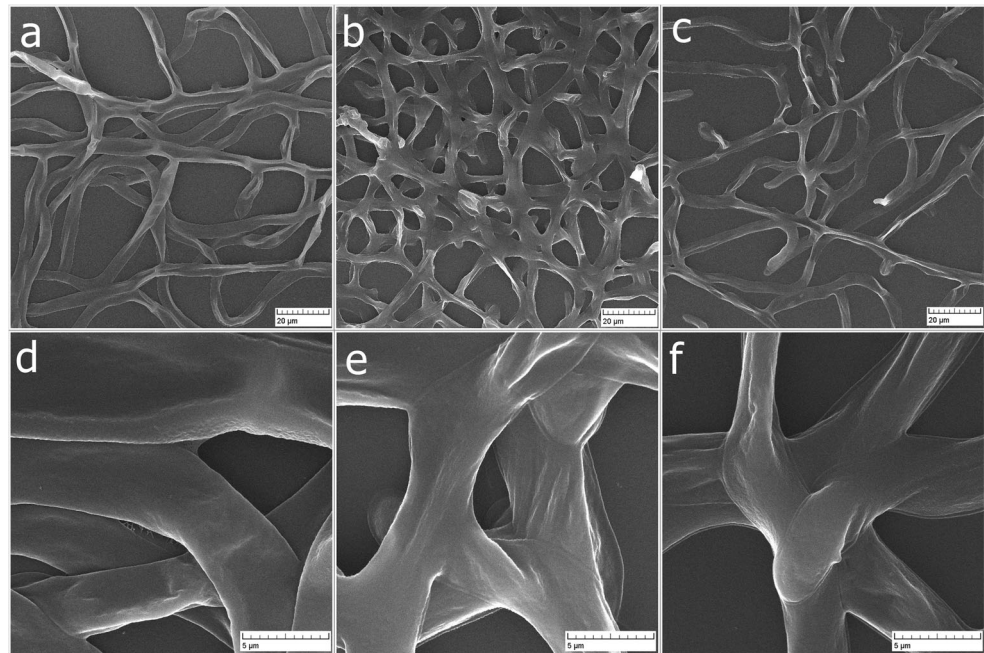
The lipid membranes are one of the first target for biologically active agents generated by the plasma. TBARS levels calculated from the molar extinction coefficient for MDA per mg of proteins increased along with the increasing duration of plasma treatment (Fig. 5). The significant increasing of TBARS ( $P < 0.05$ ) was measured in 30-s plasma-treated cells. After 90- and 180-s plasma treatments, TBARS concentration in mycelial cells was two times higher than in the control samples.

We demonstrated that after DCSBD plasma treatment, lipids were considerably oxidized by biological active substances generated by the plasma, e.g., ROS. These results were supported by fluorescent dyeing by Hoechst 33342 and PI (Fig. 6a–c).

PI, red-fluorescent intercalating agent, cannot penetrate through the membrane of live cells and can bind to DNA just in cells with permeability membrane damage. In the untreated cells (Fig. 6a), the fluorescent dye was observed in some hyphal compartments probably as result of slightly damaged cells or incomplete rinsing off excess of the dye attached to the surface of the cell wall. Nearly all hyphae treated by the plasma for 30 s were red (Fig. 6b) demonstrating that the membrane permeability was disrupted, and cells were likely dead. The decrease in fluorescence intensity of PI in 60-s treated cells (Fig. 6c) in comparison to 30-s treated cells (Fig. 6b) could be related to washing out the dye from mycelium, as the cells were not able to retain intracellular content anymore. Hyphae were evenly stained by both PI and Hoechst 33342, and the dye residues were found in all parts of the mycelium and were stronger attached to hyphal branch points (Fig. 6c, f).

Hoechst 33342 is membrane-permeant intercalating agent and binds into the minor groove of DNA preferentially to A-T regions and was used to staining living cells. On the figure obtained by fluorescent microscopy (Fig. 6d–f), Hoechst 33342 was bound to DNA in cells and the multiple nuclei in the untreated hyphae cells were observed. After 30 s of plasma treatment (Fig. 6e), nuclei were harder to observe but still detectable. Hoechst 33342 appeared more diffused throughout the cells. No nuclei were detected in 60-s plasma-treated hyphae cells (Fig. 6f), although remnants of Hoechst 33342 fluorescence remained still in the cells.

**Fig. 3** Changes in cell wall surface of *A. flavus* hyphae using SEM. Untreated (**a, d**), 60 s (**b, e**), and 180 s (**c, f**) DCSBD plasma-treated colony were observed. Total magnification was  $\times 1500$  (**a, b, c**) and  $\times 10,000$  (**d, e, f**); SEM HV 30 kV. Scale bars represent 20 (**a, b, c**) and 1  $\mu\text{m}$  (**d, e, f**)



### Plasma treatment is associated with DNA fragmentation

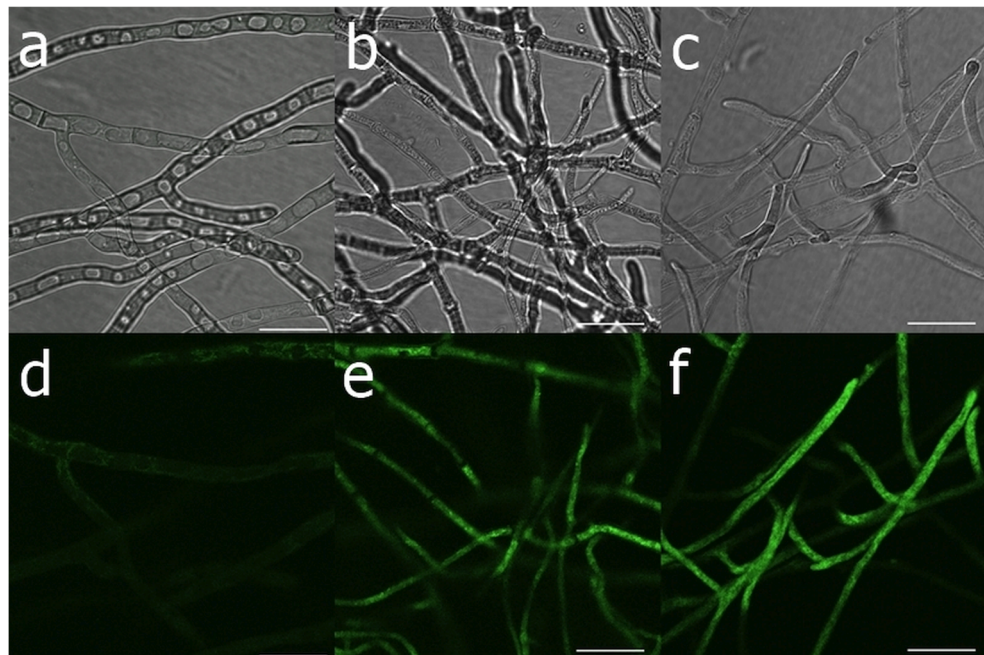
The damage of genomic DNA isolated from *A. flavus* mycelium after exposure to DCSBD plasma at different times was separated by stained agarose gel (Fig. 7). After 15 s of plasma treatment, no double strand breaks of DNA were detected and DNA had a length of more than 10,000 bp. DNA fragmentation was observed after 30 s or longer plasma treatment. Non-specific cleavage of double-strand DNA in plasma-treated

fungal cell led to formation of fragments of various lengths and was manifested as a smear on the agarose gel (Fig. 7).

### Plasma stress modulates the activity of antioxidant enzymes and the level of free non-protein thiols

Antioxidant enzymes and non-enzymatic compounds protect cell against oxidative stress by balancing the redox equilibrium. The increases of all examined antioxidant enzymes activities—CAT, SOD, and GPX, were detected after 15 and 30 s

**Fig. 4** Intracellular ROS detection by fluorescence staining of in *A. flavus* hyphae using fluorescent probe  $\text{H}_2\text{DCFDA}$ . Bright field images of hyphae: **a** untreated, **b** 30-s treated, **c** 60-s treated hyphae. Image of hyphae obtained by fluorescence microscope **d** untreated, **e** 30-s treatment, **f** 60-s treatment. Scale bar represents 25  $\mu\text{m}$



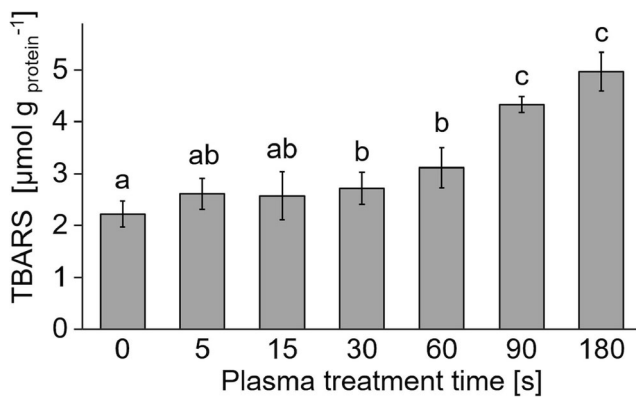


**Fig. 5** TBARS content in *A. flavus* after plasma treatment. The data were calculated to the level of proteins. Results are presented as a mean  $\pm$  SD ( $n=3$ ). Columns with different letters represent statistically significant results ( $P<0.05$ )

of plasma treatment (Fig. 8). The CAT activity was significantly increased after 15 s of plasma treatment in comparison to the control but not statistically different from the sample cultivated on medium with  $H_2O_2$  (Fig. 8a). Three-fold increase in CAT activity was detected after 30 s of plasma treatment in comparison to the control group (Fig. 8a). The GPX activity was significantly increased in order  $H_2O_2 < 15$ -s plasma treatment  $< 30$ -s plasma treatment (Fig. 8b). The smaller changes, but statistically significant, were measured in SOD activities after 30-s plasma treatment (Fig. 8c). However, decrease in SOD activity was determined in mycelium grown on medium supplemented by  $H_2O_2$  (Fig. 8c).

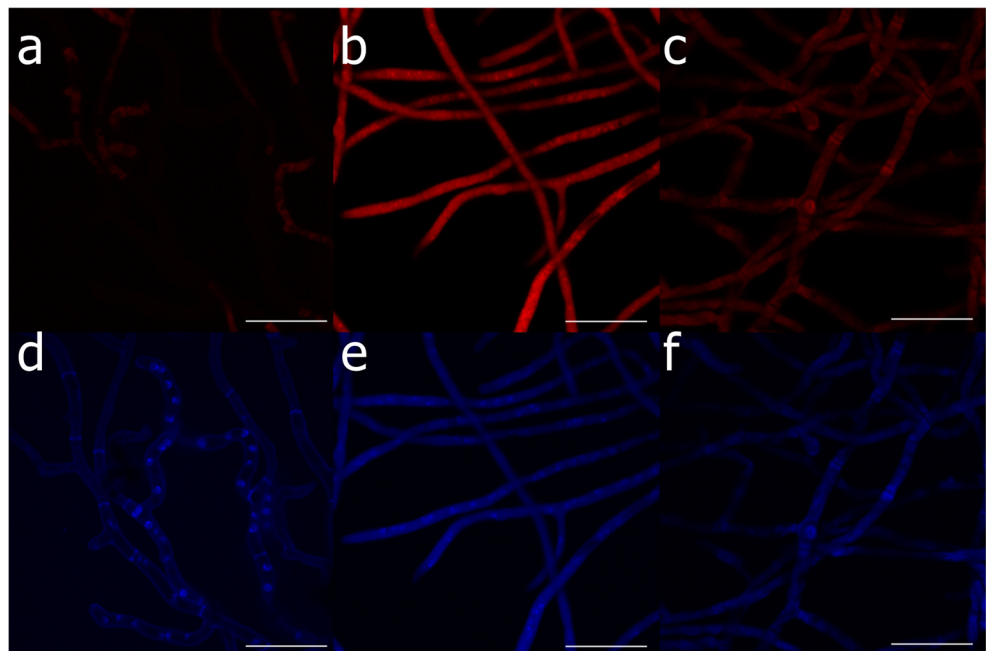
The low-molecular weight non-protein thiols significantly decreased with increasing dose of the plasma

(Fig. 8d). In samples cultivated on growth medium with  $H_2O_2$ , the total free thiol groups were found to be higher as compared with plasma-treated samples (Fig. 8d).

### Stress induced by the plasma changes composition of functional groups on surface mycelial cells

Changes in functional groups on the surface of *A. flavus* mycelium after plasma treatment were analyzed by ATR-FTIR (Fig. 9). Analysis of fungal cells by ATR-FTIR could be demanding due to carbohydrate composition that requires longer infrared wavelength (c. 10  $\mu\text{m}$ ) and leads to restrictions of spatial resolution and signal strength (Kaminskyj et al. 2008). Wide band between 3400 and 3100  $\text{cm}^{-1}$  (Fig. 9) represents OH and NH stretching vibrations. The decline in the signal intensity in this area is caused in particular by dehydration after plasma treatment and possibly also by changes in acetamido-group of chitin in the cell wall (Das et al. 2016). In addition, after longer plasma treatment, the formation of peak occurs in this area at 3280 and 3350  $\text{cm}^{-1}$ . Peaks in the region between 2800 and 3000  $\text{cm}^{-1}$  attribute to the asymmetric and symmetric stretching vibration of C-H of methylene group in fatty acid or cellulose, respectively. The enhancement of signal intensities in peaks was determined in plasma-treated cells in two distinct regions, from 950 to 1150  $\text{cm}^{-1}$  and 1200 to 1700  $\text{cm}^{-1}$ . The shorter region of the spectra corresponded to C-O stretching vibration and aromatic -CH stretching and the longer area to amide

**Fig. 6** Cell membrane permeability detected by fluorescence staining of *A. flavus* hyphae using Hoechst 33342 and PI. Hyphae **a** PI, untreated, **b** PI, 30-s treatment, **c** PI, 60-s treatment, **d** Hoechst 33342 untreated, **e** Hoechst 33342, 30-s treatment, **f** Hoechst 33342, 60-s treatment. Scale bar represents 25  $\mu\text{m}$



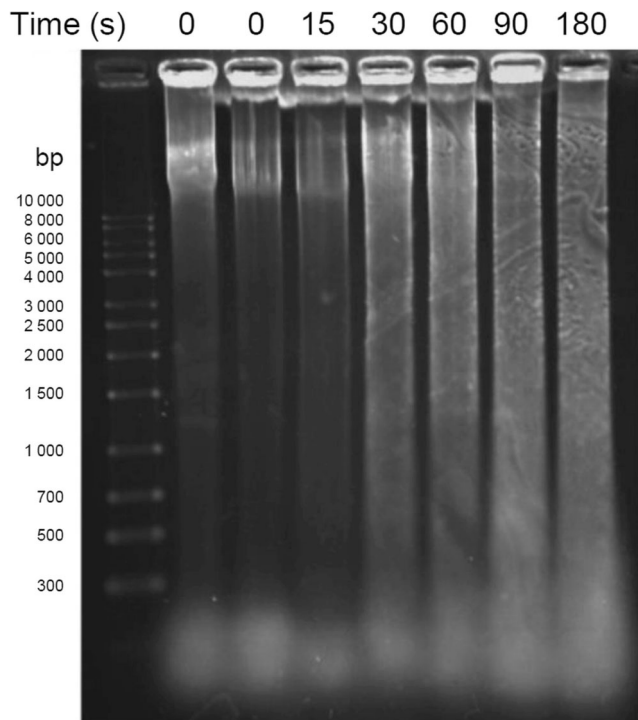


**Fig. 7** Fragmentation of DNA after plasma treatment in different time

I (C=O stretching vibration and NH deformation), amide II (NH banding), SO<sub>3</sub> group, and -CN stretching vibration of proteins. The increase in the intensity of the stretching vibrations of C=O and C-O groups on plasma-treated

samples could represent oxidation of biomolecules such as lipids and polysaccharides.

## Discussion

The effect of plasma depends on type of an organism, a cell, or a tissue type, respectively (Laroussi 2005; Mai-Prochnow et al. 2016; Bourke et al. 2017). Filamentous fungi colonizing different environmental areas develop tens of various cell types and tissues, such as vegetative hyphae, aerial hyphae, asexual and sexual spores, conidiophores, sexual female reproductive structures, chlamyospores, and arthroconidia, which differ one from another not only in structure but also in biological functions (Mcintyre et al. 2001; Bistis et al. 2003). Most of the studies that applied the cold plasma for inactivation of filamentous fungal pathogens have selectively chosen conidia, dormant reproductive non-filamentous cells, for determination of inactivation efficacy as well as much easier sample manipulation (Dasan et al. 2016a, 2016b). To investigate complexity of responses to cold plasma treatment on subcellular level, we used metabolically active mycelium of *A. flavus* grown on cellophane as a model tissue instead of dormant conidia.

The mode of plasma action in microorganisms is still subjected to thorough studies, but it has been suggested that biological reactive substances generated by the plasma (ROS, RNS, UV irradiation, and charged particles) act synergistically

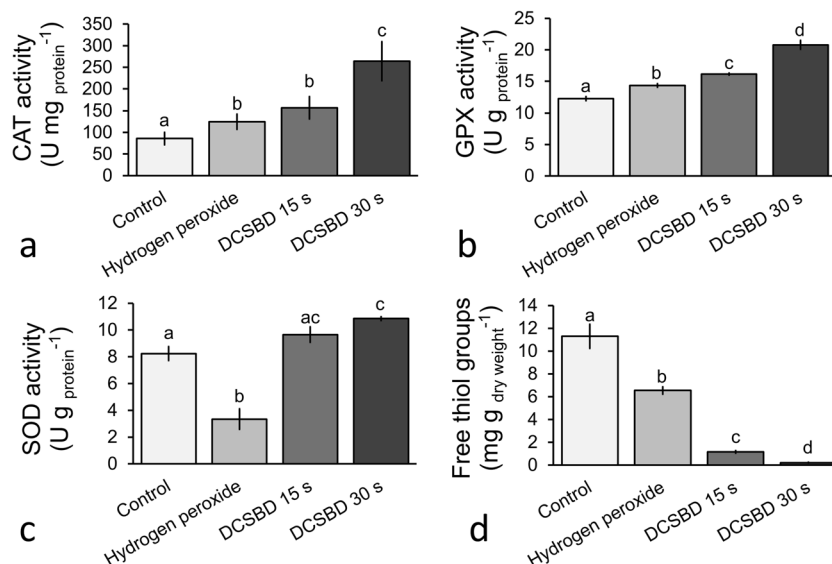
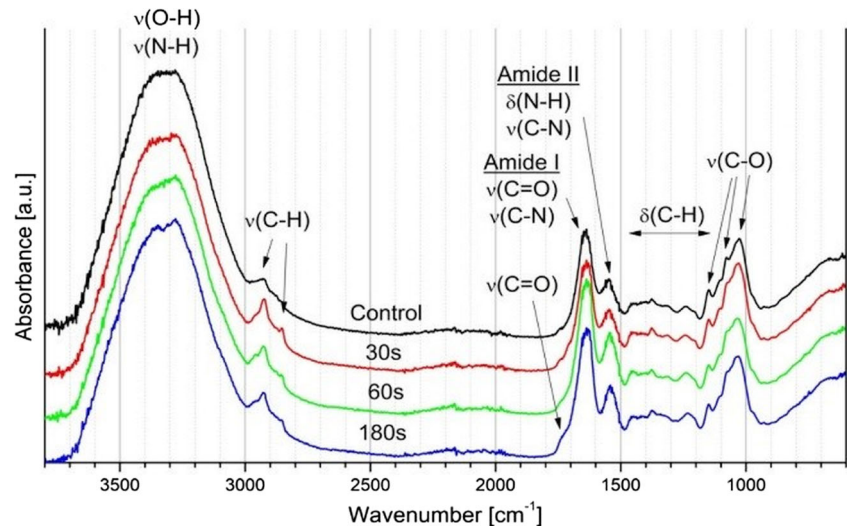


**Fig. 8** Activities of antioxidative enzymes and level of non-protein antioxidants in mycelium *A. flavus* exposed to the plasma. Plasma untreated and 15 and 30 s of DCSBD plasma-treated mycelium and mycelium cultivated on MEA medium containing 0.5-mmol l<sup>-1</sup> H<sub>2</sub>O<sub>2</sub> were used for determination **a** CAT activity, **b** GPX activity, **c** SOD

activity, and **d** non-protein low molecular weight thiols. Activities are expressed as U (μmol min<sup>-1</sup>) per mg of proteins. Amount of free thiol groups (**d**) are related to dry mycelial weight. Data are a means ± SD (*n* = 3). Columns with different letters represent statistically significant results (*P* < 0.05)



**Fig. 9** ATR-FTIR spectra of the untreated and plasma-treated (30, 60, and 180 s) *A. flavus* mycelium. Samples were analyzed using ATR-FTIR spectrometer (a.u., arbitrary units)



in microbial inactivation (Joshi et al. 2011; Alkawareek et al. 2012). The composition of plasma generated by DCSBD was measured by optical emission spectrometry, UV photometry, and mass spectrometry confirming the presence of UV irradiation, OH radicals, and different excited nitrogen and oxygen species (Kogelschatz 2003; Lazovic et al. 2008; Mošovská et al. 2018). One of the deactivation mechanisms of cold plasma is erosion of cellular surfaces through etching (Bokhorst-van de Veen et al. 2014). The fungal cell wall and plasma membrane are the first cell structures that collide with rays of radicals, electrons, excited atoms, and molecules generated by the plasma. In our study, hyphae of *A. flavus* treatment got thinner, and their surface was covered by creases (Fig. 3e, f) after 60- and 180-s plasma treatment. These changes could result from cell wall desiccation and oxidation of polysaccharides, as confirmed by ATR-FTIR analysis (Fig. 9). The morphological changes after CAPP treatment were previously observed on surface of *Aspergillus* spores. Spore aggregation, destruction of the phialide, changes in shape of cells, disruption of spore's coat, the cracks, and pores on the spore surface appeared after plasma treatment (Yoshino et al. 2013; Dasan et al. 2016a, b). Disruption of cell envelope integrity was demonstrated by increase in intensity of C=O and C-O group stretching vibrations (Fig. 9), indicating undergoing oxidation of lipid or sugar residues.

In addition to cell wall damage, the reactive species could cause perforation in cell membrane resulting in a rise in levels of secondary reactive species (Gaunt et al. 2006). The detection of membrane permeability using fluorescent detection by PI showed that nearly all hyphae treated by DCSBD plasma after 30 s or longer were stained red (Fig. 6), indicating that the membrane was unable to preserve its function which could lead to cell death. These observations were supported by lack of viability in longer plasma treatments (Fig. 2). Although we had not included fluorescent staining of 15-s plasma-treated sample in our experimental work, it is very likely that the

sample staining after shorter exposure (15 s) would have been detectable as well due to significant reduction of viability.

In this study, we showed that the amount of TBARS in fungal cells increased along with DCSBD plasma treatment time (Fig. 5). Plasma treatment induced the oxidative stress resulting in generation of MDA, a final product of polyunsaturated fatty acid peroxidation, secondary radicals, and subsequent oxidative stress. It is also very likely that when the cell wall is broken, reactive species of plasma could penetrate in the cell interior of the cell and affect enzymes and other cell macromolecules (Mai-Prochnow et al. 2016). The accumulation of intracellular ROS in plasma-treated cells of *A. flavus* was observed in vivo using a fluorescent probe, H<sub>2</sub>DCFDA (Fig. 4e, f). ROS such as OH are very reactive, but their reactivity is limited by ability to penetrate condensed layers up to a few hundred microns (Lu et al. 2016). Due to the short lifetime of ROS, the increase in intracellular ROS levels in plasma-treated cells indicated the secondary formation of ROS in cells.

The intracellular ROS are generated in eukaryotic cells during various physiological processes, e.g., during respiration, and the cells are equipped with several defense systems to protect cells against oxidative stress (Arjunan et al. 2015). These include antioxidant enzymes and non-enzymatic compounds. In this study, activity of antioxidant enzymes, CAT, SOD, and GPX, and non-protein low-molecular weight antioxidant (GSH) were studied in samples subjected to lower doses of plasma treatment (Fig. 8). The levels of reduced form of GSH significantly decreased after 30 s of plasma treatment and did not recover after plasma treatment, indicating that the cells might need other defense mechanisms including other antioxidant enzymes. We confirmed this hypothesis as we observed a significant rise in antioxidant enzyme activities. Roth et al. (2010) determined that longer plasma treatment led to a linear decrease of CAT activity in *B. subtilis*. A drop of enzyme activity is very likely associated with inactivation

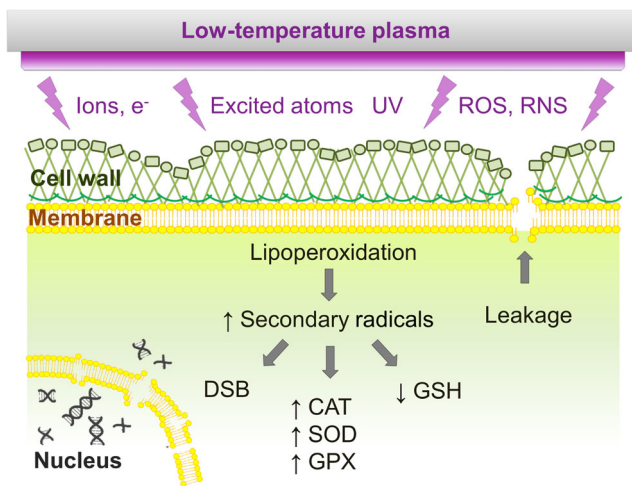


**Fig. 10** Mode of low-temperature plasma action on fungal cells. Reactive oxygen species (ROS), reactive nitrogen species (RNS), DNA double-strand breaks (DSB), catalase (CAT), superoxide dismutase (SOD), guaiacol peroxidase (GPX), reduced glutathione (GSH)

of enzymes due to changes in their structure during treatment. Both the inactivating and stimulating effects of plasma on enzymes in dose dependent manner were previously demonstrated in other samples but fungi (Roth et al. 2010; Henselová et al. 2012; Puač et al. 2014; Zhou et al. 2016).

The cell damage after higher doses of plasma is often accompanied by disintegration of organelles in eukaryotic cells (Panngom et al. 2013; Weiss et al. 2015). No nuclei were detected by Hoechst 33342 in *A. flavus* hyphae after 60 s (Fig. 6), and this was associated with DNA fragmentation (Fig. 7). The DNA analysis by gel electrophoresis at shorter periods confirmed that DNA degradation was first time detected in samples after 30-s plasma treatment, but no visible DNA degradation was observed in 15-s plasma-treated mycelium. Although no DNA fragmentation was observed after agarose gel separation in those samples treated for 15 s, viability was reduced to 10% which could indicate that cells were capable to repair damage and preserve vital functions. DNA fragmentation can occur either directly by oxidation of the deoxyribose sugar or indirectly by enzymatic cleavage of the phosphodiester backbones during repair of the oxidized bases (Joshi et al. 2011; Arjunan et al. 2015).

In conclusion, the study demonstrates outcomes of CAPP treatment on hyphal cell structure, subcellular organelles, and viability of *A. flavus* (Fig. 10). This is a first study in which we examined the impact of CAPP on young undifferentiated hyphae instead of asexual spores. Although we did not compare effect of CAPP on viability of hyphae and spores, it seems that hyphae displayed very high sensitivity to short-term treatments. CAPP treatments affected cell envelope and triggered cell defense mechanisms that were accompanied by formation of intracellular ROS and increased activity of antioxidant enzymes and compounds. The results indicated that the first interaction between plasma components and fungus occurs

on cell wall and plasma membrane causing damage to both cell structures. Compromised cell integrity then initiates number of intracellular processes such as lipoperoxidation and ROS generation. Inability to repair first damages at high CAPP treatment doses likely leads to cell content leakage and intracellular structures disintegration that culminate in cell death. Our results provide first inside into the role of hyphal envelope and subsequent cell responses during fungal interaction with CAPP reactive species. These findings could be beneficial in further studies for inactivation of various multicellular fungal species.

**Funding information** This work was supported by the Slovak Research and Development Agency under the contract no. APVV-16-0216 and by a project for the building of infrastructure for the modern research of civilization diseases, ITMS 26230120006.

## Compliance with ethical standard

**Conflict of interest** The authors declare they have no conflict of interest.

**Ethical approval** This paper does not contain any studies with human participants or animals performed by any of the authors.

## References

- Alkawarek MY, Algwari QT, Laverty G, Gorman SP, Graham WG, O'Connell D, Gilmore BF (2012) Eradication of *Pseudomonas aeruginosa* biofilms by atmospheric pressure non-thermal plasma. *PLoS One* 7:13–15. <https://doi.org/10.1371/journal.pone.0044289>
- Amaike S, Keller NP (2011) *Aspergillus flavus*. *Annu Rev Phytopathol* 49:107–133. <https://doi.org/10.1146/annurev-phyto-072910-095221>
- Amare MG, Keller NP (2014) Molecular mechanisms of *Aspergillus flavus* secondary metabolism and development. *Fungal Genet Biol* 66:11–18. <https://doi.org/10.1016/j.fgb.2014.02.008>
- Arjunan KP, Sharma VK, Ptasinaska S (2015) Effects of atmospheric pressure plasmas on isolated and cellular DNA—a review. *Int J Mol Sci* 16:2971–3016. <https://doi.org/10.3390/ijms16022971>
- Bistis GN, Perkins DD, Read ND (2003) Different cell types in *Neurospora crassa*. *Fungal Genet Rep* 50:17–19. <https://doi.org/10.4148/1941-4765.1154>
- van Bokhorst-van de Veen H, Xie H, Esveld E, Abee T, Mastwijk H, Nierop Groot M (2014) Inactivation of chemical and heat-resistant spores of *Bacillus* and *Geobacillus* by nitrogen cold atmospheric plasma evokes distinct changes in morphology and integrity of spores. *Food Microbiol* 45:26–33. <https://doi.org/10.1016/j.fm.2014.03.018>
- Bourke P, Ziuzina D, Han L, Cullen PJ, Gilmore BF (2017) Microbiological interactions with cold plasma. *J Appl Microbiol* 123:308–324. <https://doi.org/10.1111/jam.13429>
- Bradford MM (1976) A rapid and sensitive method for the quantitation of microgram quantities of protein utilizing the principle of protein-dye binding. *Anal Biochem* 72:248–254. [https://doi.org/10.1016/0003-2697\(76\)90527-3](https://doi.org/10.1016/0003-2697(76)90527-3)
- Černák M, Ráhel' J, Kováčik D, Šimor M, Brablec A, Slaviček P (2004) Generation of thin surface plasma layers for atmospheric-pressure surface treatments. *Contrib Plasma Phys* 44:492–495. <https://doi.org/10.1002/ctpp.200410069>

- Černák M, Černáková L, Hudec I, Kováčik D, Zahoranová A (2009) Diffuse coplanar surface barrier discharge and its applications for in-line processing of low-added-value materials. *Eur Phys J Appl Phys* 47:22806. <https://doi.org/10.1051/epjap/2009131>
- Conway GE, Casey A, Milosavljevic V, Liu Y, Howe O, Cullen PJ, Curtin JF (2016) Non-thermal atmospheric plasma induces ROS-independent cell death in U373MG glioma cells and augments the cytotoxicity of temozolomide. *Br J Cancer* 114:435–443. <https://doi.org/10.1038/bjc.2016.12>
- Das D, Chakraborty A, Santra SC (2016) Effect of gamma radiation on zinc tolerance efficiency of *Aspergillus terreus* thorn. *Curr Microbiol* 72:248–258. <https://doi.org/10.1007/s00284-015-0944-1>
- Dasan BG, Boyaci IH, Mutlu M (2016a) Inactivation of aflatoxigenic fungi (*Aspergillus* spp.) on granular food model, maize, in an atmospheric pressure fluidized bed plasma system. *Food Control* 70:1–8. <https://doi.org/10.1016/j.foodcont.2016.05.015>
- Dasan BG, Mutlu M, Boyaci IH (2016b) Decontamination of *Aspergillus flavus* and *Aspergillus parasiticus* spores on hazelnuts via atmospheric pressure fluidized bed plasma reactor. *Int J Food Microbiol* 216:50–59. <https://doi.org/10.1016/j.ijfoodmicro.2015.09.006>
- Deng X, Shi J, Kong M (2006) Physical mechanisms of inactivation of *Bacillus subtilis* spores using cold atmospheric plasmas. *IEEE Trans Plasma Sci* 34:1310–1316. <https://doi.org/10.1109/TPS.2006.877739>
- Devi Y, Thirumdas R, Sarangapani C, Deshmukh RR, Annapure US (2017) Influence of cold plasma on fungal growth and aflatoxins production on groundnuts. *Food Control* 77:187–191. <https://doi.org/10.1016/j.foodcont.2017.02.019>
- Ehlbeck J, Schnabel U, Polak M, Winter J, von Woedtke T, Brandenburg R, von dem Hagen T, Weltmann K (2011) Low temperature atmospheric pressure plasma sources for microbial decontamination. *J Phys D Appl Phys* 44:13002. <https://doi.org/10.1088/0022-3727/44/1/013002>
- Ellman GL (1959) Tissue sulfhydryl groups. *Arch Biochem Biophys* 82:70–77
- Fridman A (2008) Plasma chemistry. Cambridge university press
- Gaunt LF, Beggs CB, Georghiou GE (2006) Bactericidal action of the reactive species produced by gas-discharge nonthermal plasma at atmospheric pressure: a review. *IEEE Trans Plasma Sci* 34:1257–1269. <https://doi.org/10.1109/TPS.2006.878381>
- Graves DB (2014) Low temperature plasma biomedicine: a tutorial review. *Phys Plasmas* 21:80901. <https://doi.org/10.1063/1.4892534>
- Henselová M, Slovák L, Martinka M, Zahoranová A (2012) Growth, anatomy and enzyme activity changes in maize roots induced by treatment of seeds with low-temperature plasma. *Biologia* 67:490–497. <https://doi.org/10.2478/s11756-012-0046-5>
- Hojnik N, Cvelbar U, Tavčar-Kalcher G, Walsh JL, Križaj I (2017) Mycotoxin decontamination of food: cold atmospheric pressure plasma versus “classic” decontamination. *Toxins (Basel)* 9:1–19. <https://doi.org/10.3390/toxins9050151>
- Jiang F, Zhang Y, Dusing GJ (2011) NADPH oxidase-mediated redox signaling: roles in cellular stress response, stress tolerance, and tissue repair. *Pharmacol Rev* 63:218–242. <https://doi.org/10.1124/pr.110.002980.218>
- Joshi SG, Cooper M, Yost A, Paff M, Ercan UK, Fridman G, Friedman G, Fridman A, Brooks AD (2011) Nonthermal dielectric-barrier discharge plasma-induced inactivation involves oxidative DNA damage and membrane lipid peroxidation in *Escherichia coli*. *Antimicrob Agents Chemother* 55:1053–1062. <https://doi.org/10.1128/AAC.01002-10>
- Kaminskyj S, Jilkine K, Szeghalmi A, Gough K (2008) High spatial resolution analysis of fungal cell biochemistry—bridging the analytical gap using synchrotron FTIR spectromicroscopy. *FEMS Microbiol Lett* 284:1–8. <https://doi.org/10.1111/j.1574-6968.2008.01162.x>
- Kiššová I, Deffieu M, Samokhvalov V, Velours G, Bessoule JJ, Manon S, Camougrand N (2006) Lipid oxidation and autophagy in yeast. *Free Radic Biol Med* 41:1655–1661. <https://doi.org/10.1016/j.freeradbiomed.2006.08.012>
- Kogelschatz U (2003) Dielectric-barrier discharges: their history, discharge physics and industrial applications. *Plasma Chem Plasma Process* 23:1–46. <https://doi.org/10.1023/A:102247090385>
- Laroussi M (2005) Low temperature plasma-based sterilization: overview and state-of-the-art. *Plasma Process Polym* 2:391–400. <https://doi.org/10.1002/ppap.200400078>
- Laroussi M (2014) From killing bacteria to destroying cancer cells: 20 years of plasma medicine. *Plasma Process Polym* 11:1138–1141. <https://doi.org/10.1002/ppap.201400152>
- Laroussi M, Leipold F (2004) Evaluation of the roles of reactive species, heat, and UV radiation in the inactivation of bacterial cells by air plasmas at atmospheric pressure. *Int J Mass Spectrom* 233:81–86. <https://doi.org/10.1016/j.ijms.2003.11.016>
- Lazovic S, Puac N, Radic N, Hoder T, Malovic G, Ráhel' J, Černák M, Petrovic ZL (2008) Mass spectrometry of diffuse coplanar surface barrier discharge. *Publ l'Observatoire Astron Beogr* 84:401–404
- Lu X, Naidis GV, Laroussi M, Reuter S, Graves DB, Ostrikov K (2016) Reactive species in non-equilibrium atmospheric-pressure plasmas: generation, transport, and biological effects. *Phys Rep* 630:1–84. <https://doi.org/10.1016/j.physrep.2016.03.003>
- Mai-Prochnow A, Clauson M, Hong J, Murphy AB (2016) Gram positive and Gram negative bacteria differ in their sensitivity to cold plasma. *Sci Rep* 6:1–11. <https://doi.org/10.1038/srep38610>
- Mcintyre M, Müller C, Dynesen J, Nielsen J (2001) Metabolic engineering. *Adv Biochem Eng Biotechnol* 73:103–128. <https://doi.org/10.1007/3-540-45300-8>
- Mir SA, Shah MA, Mir MM (2016) Understanding the role of plasma technology in food industry. *Food Bioprocess Technol* 9:734–750. <https://doi.org/10.1007/s11947-016-1699-9>
- Misra NN, Tiwari BK, Raghavarao KSMS, Cullen PJ (2011) Nonthermal plasma inactivation of food-borne pathogens. *Food Eng Rev* 3:159–170. <https://doi.org/10.1007/s12393-011-9041-9>
- Mohamad R, Mohamed MS, Suhaili N, Salleh MM, Ariff A (2010) Kojic acid: applications and development of fermentation process for production. *Biotechnol Mol Biol Rev* 5:24–37
- Mošovská S, Medvecká V, Halászová N, Ďurina P, Valík L, Mikulajová A, Zahoranová A (2018) Cold atmospheric pressure ambient air plasma inhibition of pathogenic bacteria on the surface of black pepper. *Food Res Int* 106:862–869. <https://doi.org/10.1016/j.foodres.2018.01.066>
- ten Bosch L, Pfohl K, Avramidis G, Wieneke S, Viöl W, Karlovsky P (2017) Plasma-based degradation of mycotoxins produced by *Fusarium*, *Aspergillus* and *Alternaria* species. *Toxins (Basel)* 9:1–12. <https://doi.org/10.3390/toxins9030097>
- Panngom K, Baik KY, Nam MK, Han JH, Rhim H, Choi EH (2013) Preferential killing of human lung cancer cell lines with mitochondrial dysfunction by nonthermal dielectric barrier discharge plasma. *Cell Death Dis* 4:e642–e648. <https://doi.org/10.1038/cddis.2013.168>
- Park BJ, Takatori K, Sugita-Konishi Y, Kim IH, Lee MH, Han DW, Chung KH, Hyun SO, Park JC (2007) Degradation of mycotoxins using microwave-induced argon plasma at atmospheric pressure. *Surf Coatings Technol* 201:5733–5737. <https://doi.org/10.1016/j.surfcoat.2006.07.092>
- Puač N, Živković S, Selaković N, Milutinović M, Boljević J, Malović G, Petrović ZL (2014) Long and short term effects of plasma treatment on meristematic plant cells. *Appl Phys Lett* 104:214106. <https://doi.org/10.1063/1.4880360>
- Roth S, Feichtinger J, Hertel C (2010) Characterization of *Bacillus subtilis* spore inactivation in low-pressure, low-temperature gas plasma sterilization processes. *J Appl Microbiol* 108:521–531. <https://doi.org/10.1111/j.1365-2672.2009.04453.x>

- Ryu YH, Kim YH, Lee JY, Shim GB, Uhm HS, Park G, Choi EH (2013) Effects of background fluid on the efficiency of inactivating yeast with non-thermal atmospheric pressure plasma. *PLoS One* 8:1–9. <https://doi.org/10.1371/journal.pone.0066231>
- Sakudo A, Toyokawa Y, Misawa T, Imanishi Y (2017) Degradation and detoxification of aflatoxin B1 using nitrogen gas plasma generated by a static induction thyristor as a pulsed power supply. *Food Control* 73:619–626. <https://doi.org/10.1016/j.foodcont.2016.09.014>
- Selcuk M, Oksuz L, Basaran P (2008) Decontamination of grains and legumes infected with *Aspergillus* spp. and *Penicillium* spp. by cold plasma treatment. *Bioresour Technol* 99:5104–5109. <https://doi.org/10.1016/j.biortech.2007.09.076>
- Šimončicová J, Kaliňáková B, Kryštofová S (2017) Aflatoxins: biosynthesis, prevention and eradication. *Acta Chim Slovaca* 10:123–131. <https://doi.org/10.1515/acs-2017-0021>
- Sinha AK (1972) Colorimetric assay of catalase. *Anal Biochem* 47:389–394. [https://doi.org/10.1016/0003-2697\(72\)90132-7](https://doi.org/10.1016/0003-2697(72)90132-7)
- Su X, Tian Y, Zhou H, Li Y, Zhang Z, Jiang B, Yang B, Zhang J, Fang J (2018) Inactivation efficacy of non-thermal plasma activated solutions against Newcastle disease virus. *Appl Environ Microbiol* 81:996–1002. <https://doi.org/10.1128/AEM.03322-14>
- Suhem K, Matan NN, Nisoa M, Matan NN (2013) Inhibition of *Aspergillus flavus* on agar media and brown rice cereal bars using cold atmospheric plasma treatment. *Int J Food Microbiol* 161:107–111. <https://doi.org/10.1016/j.ijfoodmicro.2012.12.002>
- Thirumdas R, Sarangapani C, Annapure US (2014) Cold plasma: a novel non-thermal technology for food processing. *Food Biophys* 10:1–11. <https://doi.org/10.1007/s11483-014-9382-z>
- Weiss M, Gümbel D, Hanschmann EM, Mandelkow R, Gelbrich N, Zimmermann U, Walther R, Ekkernkamp A, Sckell A, Kramer A, Burchardt M, Lillig CH, Stope MB (2015) Cold atmospheric plasma treatment induces anti-proliferative effects in prostate cancer cells by redox and apoptotic signaling pathways. *PLoS One* 10:e0130350. <https://doi.org/10.1371/journal.pone.0130350>
- Yoshino K, Matsumoto H, Iwasaki T, Kinoshita S, Noda K, Iwamori S (2013) Monitoring of sterilization in an oxygen plasma apparatus, employing a quartz crystal microbalance (QCM) method. *Vacuum* 93:84–89. <https://doi.org/10.1016/j.vacuum.2013.01.009>
- Zahoranová A, Henselová M, Hudecová D, Kaliňáková B, Kováčik D, Medvecká V, Čermák M (2016) Effect of cold atmospheric pressure plasma on the wheat seedlings vigor and on the inactivation of microorganisms on the seeds surface. *Plasma Chem Plasma Process* 36:397–414. <https://doi.org/10.1007/s11090-015-9684-z>
- Zhou R, Zhou R, Zhang X, Zhuang J, Yang S, Bazaka K, Ostrikov K (2016) Effects of atmospheric-pressure N<sub>2</sub>, He, air, and O<sub>2</sub> microplasmas on mung bean seed germination and seedling growth. *Sci Rep* 6:32603. <https://doi.org/10.1038/srep32603>